CHAPTER 2

Water Adsorption on the Stoichiometric Cr_2O_3 (10$\underline{1}$2) Single Crystal Surface

2.1 Introduction

Water is one of the most studied adsorbates on well-defined metal oxide single crystal samples. The adsorption of water at solid surfaces shows a variety of applications: in geology (investigation of the forces which produce particular arrangements of water molecules in ice to understand glacial history [1]), in electrochemistry (the formation of water molecules near a metal electrode plays a key role in electrochemical reactions [2]), in physical chemistry (understanding the nature of hydrogen bonding between clustered H_2O molecules [3]), and in heterogeneous catalysis. A number of catalytic reactions including the Fischer-Tropsch synthesis of hydrocarbons, involve water as a reactant or product.

Water has a large dipole moment and lone-pair electrons, and as a result is a good electron donor and hydrogen bonder. Molecular adsorption is usually quite weak on defect-free low index surfaces. Dissociative adsorption, with a higher energy of activation for desorption, is often seen to occur at steps and defects [4]. Well-ordered single crystal surfaces have frequently been found to be unreactive towards H_2O adsorption, while powdered surfaces are easily hydroxylated. The role of surface defects (e.g. oxygen vacancies as the most commonly encountered defect type) and of non-lattice oxygen in catalyzing the dissociation of water has been demonstrated previously on metal

oxide surfaces [5,6].

The Cr_2O_3 (10$\underline{1}$2) surface is nonpolar and has the lowest energy of any low index Cr_2O_3 surface [7]. A ball model diagram of the ideal, stoichiometric surface is shown in Figure 2.1.

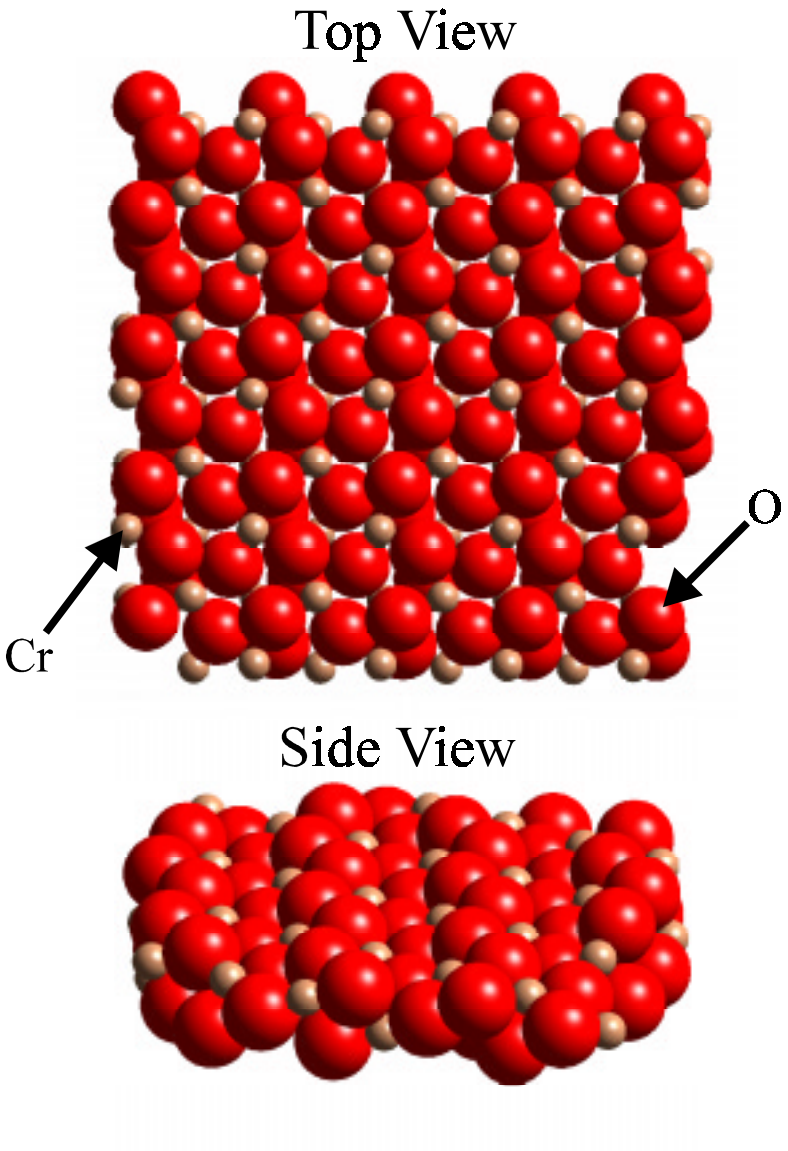

Figure 2.1: **Ball model illustration of the ideal, stoichiometric Cr_2O_3 (10$\underline{1}$2) surface.**

The topmost atomic layer of the stoichiometric Cr_2O_3 (10$\underline{1}$2) surface is composed entirely of three coordinate oxygen anions, and the second layer contains Cr^{3+} cations that are five

coordinate. The topmost oxygen anions and the second layer chromium cations each have one degree of coordinative unsaturation relative to their counterparts in the bulk. All atoms below the first two atomic layers are fully coordinated.

The primary questions of interest for H_2O adsorption on single crystal metal oxide surfaces are: (1) is the adsorption molecular or dissociative, (2) what are the dissociation products, and (3) what are the site requirements for dissociation?

2.2 Experimental

All experiments were conducted in an ion-pumped, single chamber, stainless steel ultrahigh vacuum (UHV) system equipped with a Perkin Elmer model 15-155 single-pass cylindrical mirror analyzer for Auger electron spectroscopy (AES), a broad beam Ar^+ ion gun for sample cleaning, and a set V.G. 3-grid reverse view LEED optics. The base pressure of the UHV system is 1×10^{-10} Torr. AES experiments were performed using an incident electron beam energy of 5 keV with spectra being collected in an N(E) mode and differentiated numerically. An Inficon Quadrex 200 mass spectrometer was used for thermal desorption spectroscopy (TDS).

Gas exposures were performed by backfilling the chamber through a variable leak valve. Aldrich HPLC grade H_2O was used following degassing with a number of freeze-pump-thaw cycles. A 2 K/s linear temperature ramp was used in all TDS experiments. The low heating rate was used to minimize the possibility of thermal fracture of the ceramic Cr_2O_3 sample. The mass spectrometer was equipped with a quartz skimmer to minimize the contribution to the desorption signal from the sample hardware.

The single crystal Cr_2O_3 sample was oriented using Laue backreflection, and mechanically polished to within 1° of the (10$\underline{1}$2) plane. The sample has an exposed surface area of approximately 77 mm^2 and an average thickness of 1 mm. The sample was mounted on a tantalum holder which acted as an indirect heating and cooling source. The sample holder assembly was mechanically attached to an XYZ rotary sample manipulator. The sample temperature was monitored using a type K thermocouple attached, through a hole in the back of the sample holder, to the rear of the sample using AREMCO #569 ceramic cement. The sample could be cooled to 130 K, using a liquid

nitrogen cooled heat sink, and resistively heated to 1100 K.

The clean, nearly-stoichiometric Cr_2O_3 (10$\underline{1}$2) surface was obtained following ion bombardment with 2 keV Ar^+ and annealing at 900 K for five minutes in UHV [8]. The clean surface exhibits a (1x1) low-energy electron diffraction (LEED) pattern. XPS analysis confirms the presence of chromium in the 3^+ valence state with an O:Cr ratio of 1.5 ± 0.1 [9]. The clean surface O:Cr ratio as measured using Auger electron spectroscopy (AES) at 873 K and corrected for atomic sensitivities is 0.70 ± 0.03. AES must be done at high temperature where the material conductivity is sufficient to prevent charging by the primary electron beam. Overlap of the primary oxygen and chromium peaks and distortion of the peak shapes at elevated temperatures makes it difficult to obtain a more accurate estimate of the O:Cr ratio with AES. However, the ratio of 0.70 is characteristic of a stoichiometric surface as seen by comparison to the XPS results. Details of the surface characterization are found elsewhere [8].

2.3 Results

2.3.1 Thermal Desorption Spectroscopy

The adsorption of water was studied on the stoichiometric Cr_2O_3 (10$\underline{1}$2) surface using thermal desorption spectroscopy (TDS). The surface was exposed to water at 163 K and heated linearly at 2 K/s to 725 K. H_2O was the only desorption product observed in TDS; no H_2 or O_2 was detected. The high background of H_2 in the vacuum system may have limited the ability to detect a small amount of H_2 desorption.

A series of thermal desorption traces following adsorption of H_2O are shown in Figure 2.2.

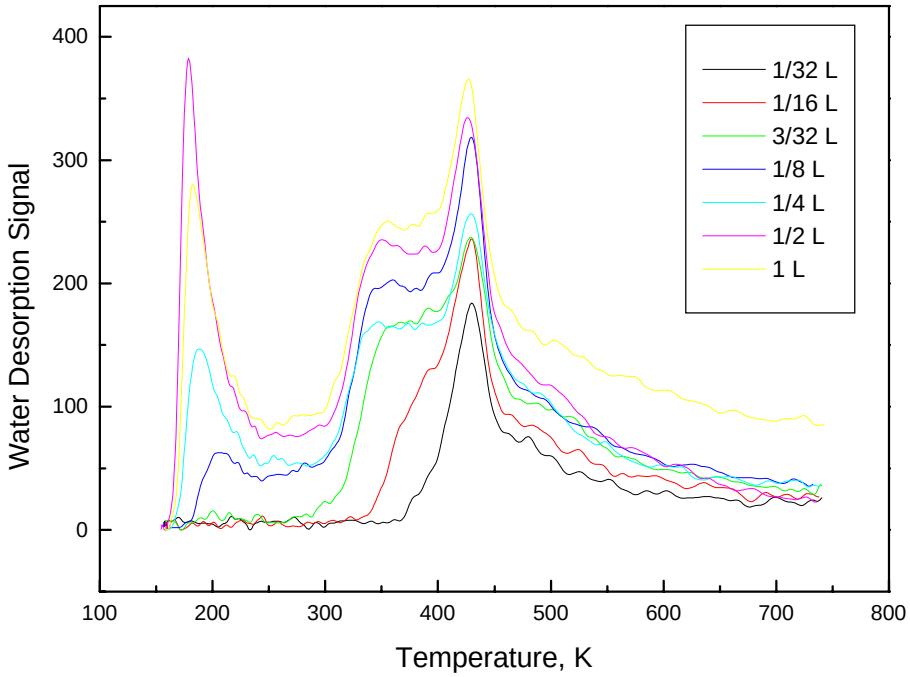

Figure 2.2: Thermal desorption traces for water following adsorption at 163 K on the nearly stoichiometric Cr_2O_3 (10$\underline{1}$2) surface.

At the lowest exposures, up to 0.06 L, the predominant feature is sharp with a peak temperature, T_P, of 428 K. At an exposure of 0.09 L, a broad shoulder begins to form on

the low temperature side of the 428 K feature. The desorption temperature of this second feature is between 348-351 K. At increasing coverages an additional low temperature feature was observed. The low temperature feature was observed, beginning at an exposure of 0.13 L, with a peak temperature of 205 K. The temperature of this low temperature feature decreased with increasing coverage to a final value of 183 K at a 1 L exposure.

The low temperature feature results primarily from desorption from non-sample surfaces, including the shims, and sample support hardware. No multilayer water desorption feature was observed. Multilayer ice temperatures of 160 K-165 K have been reported previously on a number of metal surfaces [5] and on other well defined oxide surfaces [10,11]. In this study the H_2O dosing temperature, 163 K, is probably too high to form water multilayers on Cr_2O_3 ($10\underline{1}2$).

A saturation coverage of H_2O is reached at an exposure of 0.13 L, as indicated by a constant integrated area under the two high temperature features, which result from H_2O desorption from the sample. H_2O desorption peak areas are shown in Figure 2.3. The kinetic theory of gases can be used to estimate an upper limit for the water coverage. An exposure of 0.13 L corresponds to an uptake of 6.0×10^{13} water molecules/cm^2, assuming a unity sticking coefficient. The surface exposes 4.85×10^{14} Cr atoms/cm^2 assuming an ideal, stoichiometric termination of the bulk. If a monolayer of water is defined as one water molecule per surface chromium atom, the desorption features at 350 K and 428 K represent only 12% of a monolayer or less.

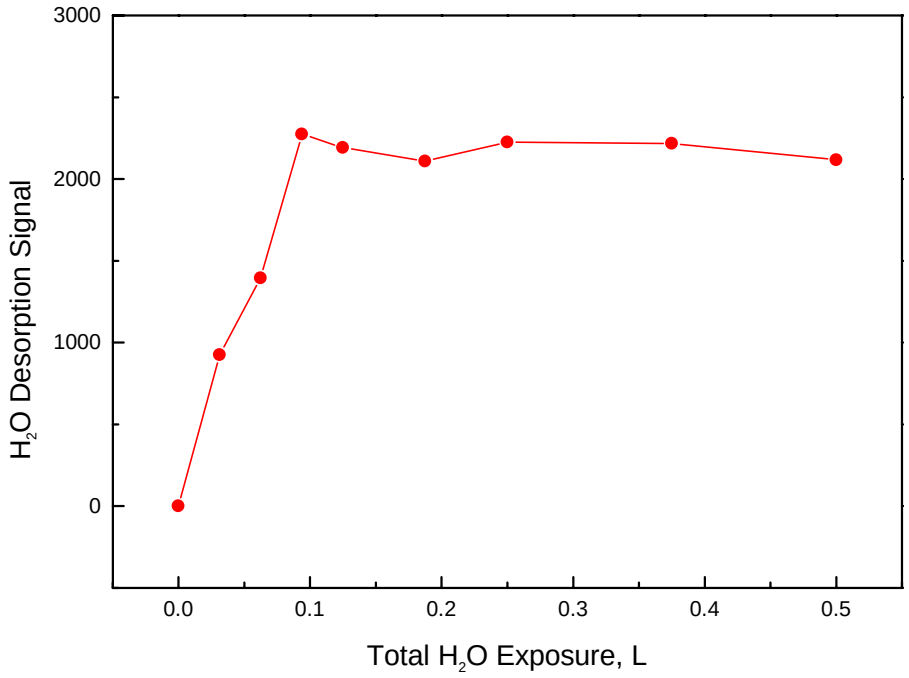

Figure 2.3: H_2O desorption peak areas following adsorption at 163 K on the nearly stoichiometric Cr_2O_3 (10$\underline{1}$2) surface.

The two high temperature features, 428 K and 350 K, appear first-order with nearly constant peak temperatures with changing coverages for doses up to 1 L [12]. Using the Redhead equation [12] and assuming a normal first-order pre-exponential of 10^{13} s^{-1} the first-order activation energy of desorption for the feature at 428 K is 27.1 kcal/mol and 22.0 kcal/mol for the 350 K feature.

The adsorption of deuterium oxide (D_2O) was also studied on the stoichiometric Cr_2O_3 (10$\underline{1}$2) surface using TDS. The surface was exposed to D_2O at 163 K and heated linearly at 2 K/s to 725 K. D_2O was the only desorption product observed in TDS. No kinetic isotope effect is observed for D_2O, with desorption occurring over the same temperature ranges observed previously for H_2O. Figure 2.4 shows a comparison of the thermal desorption traces for water and D_2O following a 1/4 L exposure.

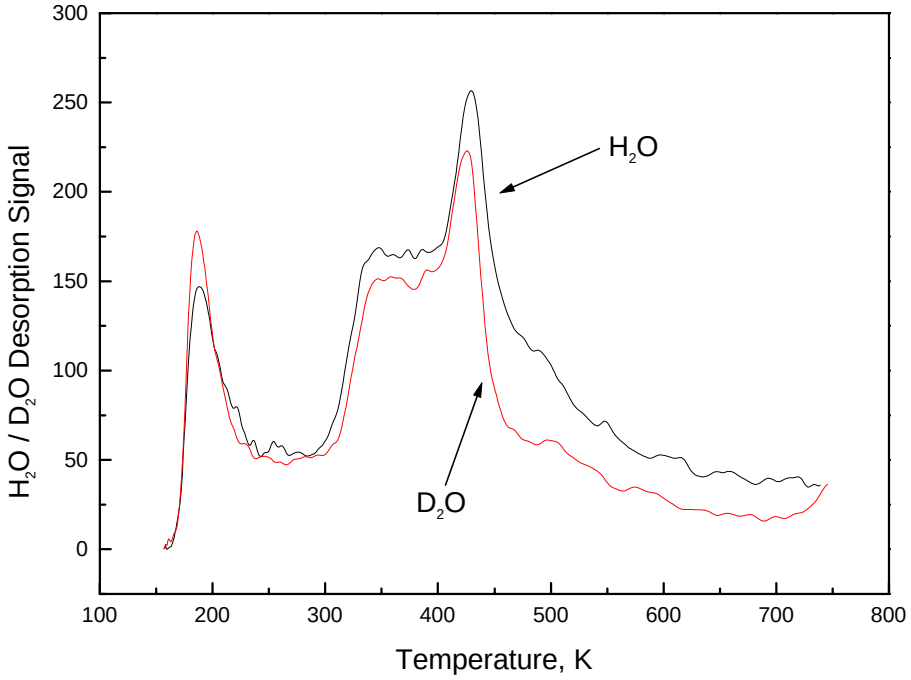

Figure 2.4: Thermal desorption traces for a 1/4 L exposure of D_2O and H_2O following adsorption at 163 K on the nearly stoichiometric Cr_2O_3 (10$\underline{1}$2) surface.

Using the Redhead equation and assuming a normal first-order pre-exponential factor of 10^{13} sec^{-1} [12] an increase in the desorption temperature of ~19 K is anticipated due to a primary kinetic isotope effect, assuming a difference in the zero-point vibrational energies (ΔE_0) of 1.2 kcal/mol [13] for OH versus OD bonds. Similar desorption temperatures for H_2O and D_2O indicates that the rate-limiting step for desorption does not involve the formation or cleavage of an OH or OD bond.

2.3.2 Ultraviolet Photoelectron Spectroscopy

UPS experiments are useful in identifying surface intermediates and distinguishing between molecular and dissociative adsorption of water. Because of the insulating nature of Cr_2O_3, UPS on the Cr_2O_3 (10$\underline{1}$2) surface was possible only well above

room temperature, 700-800 K, where sufficient carriers are present to stabilize charging. UPS of water, with a maximum desorption temperature of 428 K on Cr_2O_3 (10$\underline{1}$2), cannot be studied at the elevated temperatures required for the single crystal Cr_2O_3 (10$\underline{1}$2) surface.

2.4 Discussion

The high temperatures of the desorption features at 350 K and 428 K indicates that the desorption is likely due to the recombination of dissociated water. Disproportionation of surface OH^- groups ($2OH^- \rightarrow H_2O + O^{2-}$) to form water has been proposed on the following of oxides: NiO (100) [14], V_2O_3 [15], Ti_2O_3 [16], TiO_2 (110) [11], SnO_2 (110) [17], Cu_2O (100) [10], and Cu_2O (111) [18]. The H_2O desorption temperatures for disproportionation of OH ranges from 300 K on Cu_2O (100) [10] to 435 K on SnO_2 (110) [16]. UPS studies on thin film Cr_2O_3 (111) indicate that molecular water is primarily removed from the surface at 160 K, most likely due to desorption of a multilayer, and completely removed by 250 K [19]. The formation of OH groups on a Cr_2O_3 (111) thin film following exposure of H_2O at 100 K has also been confirmed using UPS [19]. The OH groups remain on a Cr_2O_3 (111) thin film up to annealing temperatures on the order of 500 K [19]. The 350 K and 428 K desorption temperatures fall in the range of temperatures, 300 K to 435 K, observed previously for OH disproportionation on a number of oxide surfaces [10,11,14-17], and in the range of temperatures, 250 K to 500 K, where OH is the only surface species remaining on a thin film Cr_2O_3 (111) sample exposed to H_2O [19].

Approximately, 0.12 monolayers of water dissociate on a clean, nearly stoichiometric Cr_2O_3 (10$\underline{1}$2) surface. Cappus, *et. al.* believe that OH groups are formed exclusively at defect sites on Cr_2O_3 (111) thin film surfaces [19]. If a similar phenomenon occurs on Cr_2O_3 (10$\underline{1}$2), the coverage of dissociated water provides an estimate of the defect density at the surface equivalent to 12% of the surface Cr sites. One suggested way to test this assumption is by the intentional introduction of defects via

ion bombardment. It is noted, however, that similar behavior has been observed on Cu_2O (100) [10] and TiO_2 (110) [20] where only a small fraction of a monolayer of water dissociates. On Cu_2O (100) this behavior is not associated with defects, and the cause of the behavior is not understood [10].

The kinetics associated with desorption of water at 350 K and 428 K are first-order, indicating that the rate-limiting step for desorption is not simply the reaction between two OH groups, a second-order process. The first-order kinetics suggest that the rate-limiting step is the decomposition of the OH surface intermediate. However, the lack of a primary isotope effect indicates that OH or OD bond breaking is not rate limiting. One possible explanation for the observation is a rate-limiting step involving Cr-O bond breaking to form a freely diffusing surface OH species. In a similar vein, it has been suggested that Cu^+-O bond breaking may be rate-limiting in the first-order recombination of dissociated water on Cu_2O (100) [10]. Clearly, however the details of these processes are not well understood.

2.5 Conclusions

Adsorption of water on the stoichiometric Cr_2O_3 (10$\underline{1}$2) was studied. Water was the only desorption product observed. Adsorption is primarily dissociative following exposure to water at 163 K. The low temperature feature, 183 K to 205 K, results from desorption from non-sample surfaces. Desorption at 350 K and 428 K is due to the recombination of dissociated water.

2.6 References

[1] P. A. Shumskii, Principles of Structural Glaciology (Dover, New York, 1964).

[2] L.R. Faulkner, *J. Chem. Ed.* **60** (1983) 262; E. Gileadi, Interfacial Electrochemistry (Addison-Wesley, Reading, MA 1975).

[3] S.Kittaka, T. Sasaki, N. Fukuhara, and H. Kato, *Surface Science* **282** (1993) 255.

[4] V. E. Henrich and P.A. Cox, The Surface Science of Metal Oxides (Cambridge, New York, 1994).

[5] P. A. Thiel and T. E. Madey, *Surface Science Reports* **7** (1987).

[6] V.E. Henrich, *Reports on Progress in Physics* **48** (1985) 1481; V.E. Henrich, *Prog. Surf. Sci.* **9** (1979) 143.

[7] P. J. Lawrence, S. C. Parker, and P. W. Tasker, *J. Amer. Ceram. Soc.* **71** (1988) 389.

[8] S. York and D. F. Cox, manuscript in preparation.

[9] M. W. Abee and D. F. Cox, unpublished data.

[10] D. F. Cox and K. H. Shulz, *Surface Science* **256** (1991) 67.

[11] M. B. Hugenschmidt, L. Gamble, and C. T. Campbell, *Surface Science* **302** (1994) 329.

[12] P. A. Redhead, *Vacuum* **12** (1962) 203.

[13] K. J. Laidler, Chemical Kinetics (Harper and Row, New York, 1987).

[14] J. M. McKay and V. E. Henrich, *Phys. Rev. B* **32** (1985) 6764.

[15] R. L. Kurtz and V. E. Henrich, *Pys. Rev. B* **28** (1983) 6699.

[16] R. L. Kurtz and V. E. Henrich, *Phys. Rev. B* **26** (1982) 6682.

[17] V. A. Gercher and D. F. Cox, unpublished data.

[18] A.C. Christiaen and D. F. Cox, Unpublished Data (Thesis).

[19] D. Cappus, C. Xu, D. Ehrlich, B. Dillmann, C.A. Ventrice Jr., K. Al Shamery, H. Kuhlenbeck, and H.J. Freund, *Chemical Physics* **177** (1993) 533.

[20] R. L. Kurtz, R. Stockbauer, T. E. Madey, E. Roman, and J. L. De Segovia, *Surface Science* **218** (1989) 178.